10

Optical and photoluminescent properties in the ultraviolet and visible spectral range of ZnO thin films created using corpuscular-photonic technology

© L.V. Grigoryev[1,2], A.A. Semenov[2]

[1] St. Petersburg State University, St. Petersburg, Russia
[2] St. Petersburg State Electrotechnical University „LETI", St. Petersburg, Russia

e-mail: lvgrigoryev@mail.ru

Received September 10, 2024
Revised September 10, 2024
Accepted October 27, 2024

The investigated structural, optical and photoluminescent properties of ZnO thin films produced by various corpuscular-photonic technologies, such as reactive ion-plasma sputtering, pulsed electron beam evaporation and laser ablation. The results of X-ray structural analysis of zinc oxide films synthesized on KU-1 quartz substrates are presented. Transmission spectra, reflectance spectra, absorption spectra and spectral dependence of photoluminescence of ZnO thin films in the ultraviolet and visible ranges of the spectrum are presented.

Keywords: zinc oxide, diffraction pattern, reactive ion-plasma sputtering, pulsed electron beam sputtering, laser ablation, transmission spectrum, reflectance spectrum, photoluminescence spectrum.

DOI: 10.61011/EOS.2024.10.60059.7064-24

Introduction

The structural and optical properties of zinc oxide (ZnO) thin films attract much research attention at present. This interest stems from the possibility of fabrication of UV photodetectors, photo-controlled acousto-electronic devices, planar acousto-optic microdevices, and photo-sensitive magneto-optic devices on the basis of thin-film structures with a ZnO layer [1–3]. Such microstructures with ZnO (a semiconducting piezoelectric) may operate as part of fiber-optic and planar devices with applications in radio photonics, magnetic optics, functional electronics, and microphotonics. The feasibility of production of an optically controlled microelectronic structure for sensors and acousto-electronic, acousto-optic, magneto-optic, and radio photonics devices necessitates a comprehensive study of the structural and optical properties of a thin ZnO film.

In the present study, we report the results of examination of structural, optical, and photoluminescent properties of thin-film ZnO structures formed on high-purity KU-1 quartz substrates.

Sample fabrication

Thin ZnO films were fabricated on the surface of polished KU-1 quartz wafers using different corpuscular-photonic methods: reactive ion-plasma sputtering, pulsed electron-beam evaporation, and laser ablation [4]. The surface of quartz wafers was polished to class 14 smoothness. Prior to the application of a zinc oxide layer to the quartz substrate surface, all substrates were cleaned of organic contaminants by rinsing in polar and non-polar solvents; after that, the substrates were rinsed in deionized water with a resistivity above 1.0 MΩ. All quartz substrates were also subjected to ion bombardment (ion assistance) in argon-oxygen plasma to remove residual trace contamination and enhance the adhesion of deposited zinc oxide. The working volume of the setup, where the substrates were mounted, was then evacuated to the working pressure. Zinc oxide layers were formed on the substrate surface by reactive ion-plasma sputtering of a high-purity metal target, by pulsed electron-beam evaporation of a target pellet, or by pulsed laser ablation of a target pellet made of high-purity ZnO powder.

Ion-plasma sputtering of the target was performed using a DC magnetron sputtering setup. A zinc oxide film was synthesized in a gas atmosphere containing 20% O_2 and 80% Ar_2. The pressure of the $O_2 + Ar_2$ gas mixture in the process of zinc oxide sputtering in the reactor did not exceed 1.01 Pa. The quartz substrate was heated by an infrared lamp. The quartz substrate temperature was maintained at 425 K. The thickness of the ZnO film formed on the polished quartz substrate was controlled indirectly by monitoring the frequency change of a high-frequency quartz generator (microbalance).

A LEYBOLD setup was used for electron-beam deposition of a ZnO layer. In order to reduce the influence of gas atmosphere in the jig on the quality of the synthesized zinc oxide film, the mode of pulsed sputtering of a target pellet made of pressed high-purity zinc oxide powder without any additives [4] was used. The beam current was 150 mA, and the accelerating voltage was 1.8 kV. The electron-beam gun featured a hot tungsten cathode, circuits for rotating the electron beam in a magnetic field, and a circuit for scanning the beam over the sputtered target. The pressure in the reactor volume of the setup did not exceed 10^{-3} Pa.

The quartz substrate temperature was maintained at 425 K. The quartz substrate was heated by irradiating it with an infrared lamp. As before, the zinc oxide film thickness was monitored with the use of a quartz microbalance.

To reduce the influence of composition of the residual gas atmosphere in the reaction zone of the chamber on the morphology and phase composition of thin ZnO films, their synthesis by laser ablation was carried out in the pulsed mode of target irradiation by the laser. The laser beam was scanned over the target surface to prevent target melting, impingement of large melt droplets on the substrate, and target burn-through. The working volume of the reactor, which was used to synthesize zinc oxide films, was evacuated to a residual pressure below 1.01 Pa with a two-loop oil-free pumping system. A pulsed DPSS Nd:YAG laser of an original design operating at the fundamental wavelength of 1064 nm was used to perform laser ablation. The laser pulse repetition rate could be adjusted from 100 to 20 Hz in the film deposition process. The laser pulse energy was 740 mJ. The laser pulse duration was 10–12 ns. The DPSS laser was operated in the giant-pulse mode. These pulses were generated using a cavity of an industrial laser modified to include an intracavity acousto-optic modulator of a proprietary design made of paratellurite. The collimated laser flux was introduced into the reaction chamber through a sapphire window. Laser radiation was focused onto the ZnO target surface to a spot with a diameter no greater than 600 μm. The distribution of laser radiation power over the beam section was Gaussian. The quartz substrate temperature was maintained at 425 K. As before, the quartz substrate was heated by irradiating it with an infrared lamp. The film thickness was monitored in the process of growth with a quartz microbalance.

Zinc oxide layers 3.0 μm in thickness were formed on the substrate surface as a result of corpuscular-photonic deposition.

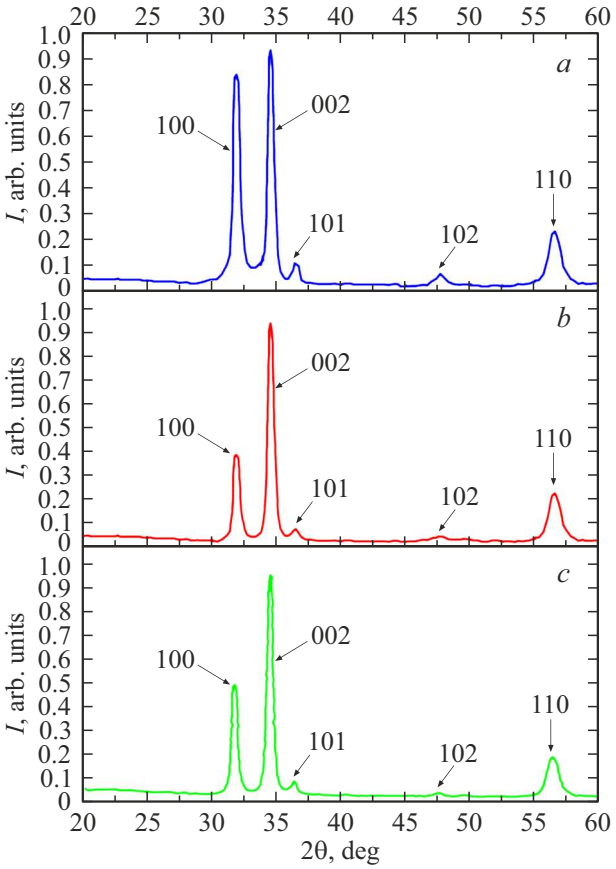

Figure 1. X-ray diffraction pattern of thin ZnO films fabricated using different corpuscular-photonic methods: *a* — laser ablation; *b* — pulsed electron-beam evaporation; and *c* — reactive ion-plasma sputtering.

Experimental results

X-ray diffraction studies were carried out using a DRON-3M diffractometer with CuK_α = 1.542 Åradiation; the anode voltage of the X-ray tube was 27 kV. Scanning was performed within the range of Bragg angles 2θ varying from 20 to 60°. The scan pitch was $\Delta 2\theta = 0.05°$. The signal accumulation time at a measurement point was 10 s.

The diffraction patterns of ZnO films fabricated by laser ablation, pulsed electron-beam evaporation, and reactive ion-plasma sputtering are presented in Figs. 1, *a*–*c*, respectively. Thin ZnO films formed by all three methods have a low density of structural defects located both in the bulk of a film and at the quartz–zinc oxide interphase boundary. This agrees well with the results of X-ray diffraction studies of thin ZnO films presented in [5–7]. All diffraction patterns contain a high-intensity diffraction maximum typical of hexagonal zinc oxide (002), which is indicative of a high degree of structural perfection of the synthesized thin zinc oxide films. In addition, the high intensity of the (002) peak also provides a clear indication of the presence of a distinct axial texture in the ZnO thin film in the direction perpendicular to the substrate surface [5–7].

Having processed the X-ray diffraction data by the Selyakov–Scherrer method [8], we found that the sizes of zinc oxide nanocrystallites in the ZnO film formed by ion-plasma sputtering did not exceed 15 nm. In the case of the ZnO film formed by pulsed electron-beam evaporation, the sizes of zinc oxide nanocrystallites did not exceed 13 nm. Zinc oxide nanocrystallites in the bulk of the ZnO film synthesized by laser ablation were no larger than 11 nm.

The highest (100) peak intensity was observed in films fabricated by laser ablation, while the lowest intensity corresponds to films produced by electron-beam evaporation.

Positional shifts of reflection maxima visible in the diffraction patterns of the studied samples and changes in their intensity are probably attributable to an increase in the interplanar distance in the nanocrystalline zinc oxide film. This variation of interplanar distance may be induced by tensile elastic stresses emerging in the ZnO film due to a strong difference in lattice constants between the synthesized semiconductor film and the quartz substrate.

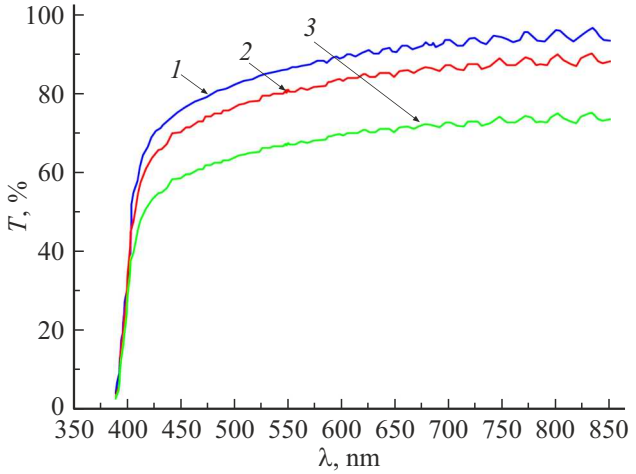

Figure 2. Transmittance spectra of ZnO films. The ZnO layer is produced by: *1* — laser ablation; *2* — pulsed electron-beam evaporation; and *3* — reactive ion-plasma sputtering.

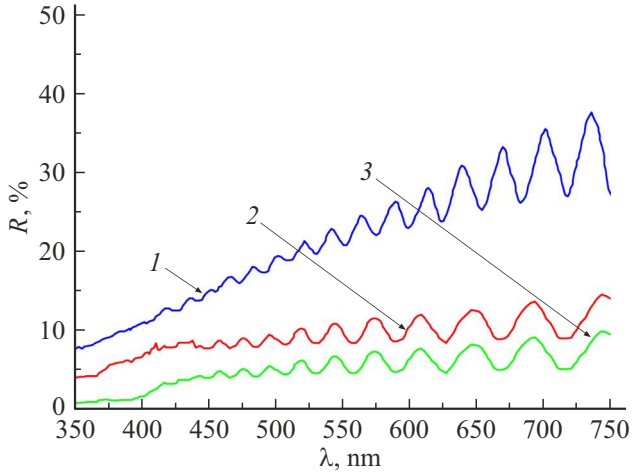

Figure 3. Reflectance spectra of ZnO films. The ZnO layer is produced by: *1* — laser ablation; *2* — pulsed electron-beam evaporation; and *3* — reactive ion-plasma sputtering.

A close correlation in the angular position of the (002) reflection peak in all the examined cases follows from the analysis and comparison of literature data [5,6] on diffraction patterns of ZnO films synthesized by high-frequency sputtering of a zinc oxide ceramic target and the diffraction patterns discussed above. It should be noted that the zinc oxide film synthesized by high-frequency sputtering of a ceramic target [5] lacked diffraction maxima (100), (101), (102), and (110) that are present in the diffraction patterns of samples produced by ion-plasma sputtering of a metal target, pulsed electron-beam evaporation, and pulsed laser ablation.

The transmittance and reflectance spectra were studied within the wavelength range from 375 to 800 nm with a Perkin Elmer Lambda 650 spectrometer. Measurements were carried out at room temperature. Transmittance spectra $T(\lambda)$ of zinc oxide are shown in Fig. 2. Curve *1* corresponds to $T(\lambda)$ for the ZnO film produced by pulsed laser ablation. Curve *2* corresponds to $T(\lambda)$ for the ZnO film produced by pulsed electron-beam evaporation. Curve *3* corresponds to $T(\lambda)$ for the ZnO film produced by ion-plasma sputtering of the metal target. It follows from these spectra that the transmittance varies from 38 to 94% within the wavelength range of 400–800 nm. The transmittance spectra of all three films also feature oscillations caused by the interference of light in thin films. The $T(\lambda)$ dependences for all the studied zinc oxide films are matching within the spectral band from 375 to 400 nm; differences emerge only after 400 nm. The transmittance of all three zinc oxide films increases sharply (although at different rates) within the 400–428 nm spectral band. At wavelengths greater than 430 nm, this growth ceases in the film synthesized by ion-plasma target sputtering and continues in the films synthesized by electron-beam evaporation and laser ablation. The highest rate of transmittance growth within the 400–450 nm wavelength band was found in the zinc oxide film synthesized by laser ablation. As the wavelength increases further to 625 nm, the transmittance of the film synthesized by laser ablation continues to grow at the same rate, remaining 10–12% higher than the $T(\lambda)$ curve for the film synthesized by electron-beam evaporation. The transmittance of the film synthesized by laser ablation reaches 90% at 625 nm and increases smoothly to 94% within the 625–800 nm spectral band. The transmittance of the film synthesized by pulsed electron-beam evaporation increases smoothly from 75 to 82% within the 450–800 nm spectral band.

The reflectance spectra for all the three studied ZnO films are shown in Fig. 3. Curve *1* corresponds to spectral dependence $R(\lambda)$ of the film synthesized by pulsed laser ablation, curve *2* corresponds to $R(\lambda)$ of the film synthesized by pulsed electron-beam evaporation, and curve *3* corresponds to $R(\lambda)$ of the film synthesized by ion-plasma sputtering of the target. It should be noted that all $R(\lambda)$ dependences feature oscillations caused by the interference of light in thin films. Dependence $R(\lambda)$ for the film synthesized by pulsed laser ablation is monotonically increasing and may be approximated by two linear functions: the reflectance increases quasi-linearly from 9 to 15% within the 350–550 nm spectral band and continues to grow quasi-linearly to 26% at a lower rate (with a smaller angle of inclination to the wavelength axis) within the 556–800 nm spectral band. Dependence $R(\lambda)$ of the film synthesized by ion-plasma sputtering of the metal target has a complex form and consists of three sections:$R(\lambda)$ increases linearly from 1.8 to 2.6% within the spectral band from 350 to 390 nm and jumps to 4.4% within the 390–426 nm band; at longer wavelengths of 450–800 nm, $R(\lambda)$ undergoes a monotonic quasi-linear increase to an average value of 4.6% with significant oscillations caused by the interference effect in the thin film. The $R(\lambda)$ dependence of the film synthesized by pulsed electron-beam evaporation features two sections.

Curve *2* in Fig. 3 increases linearly from 4.8 to 7.4% within the 350–435 nm spectral band continues to grow quasi-linearly to 8.3% within the 435–800 nm band. This $R(\lambda)$ plot is also characterized by significant oscillations attributable to thin-film interference. The refraction index of the examined ZnO films was determined to be 2.36 in a joint analysis of the $T(\lambda)$ and $R(\lambda)$ dependences and interference bands in the transmittance and reflectance spectra of these films. The obtained value is close to the one determined for the zinc oxide film synthesized by reactive magnetron sputtering [5,6].

The spectral dependences of transmittance, absorptance, and refraction index of a film in the wavelength region where interference is not observed are related [9,10] in the following way:

$$T_0 = \frac{(1-R)^2[1+(\lambda\alpha/4\pi n)^2]}{\exp(\alpha d) - R^2\exp(-\alpha d)}. \quad (1)$$

The spectral dependence of the film transmittance in the presence of interference takes the form [9]

$$T - \frac{(1-R_{12})^2}{1+R_{12}^2 - 2R_{12}\cos(4\pi nd/\lambda)}, \quad (2)$$

where $R_{12} = \left(\frac{n-1}{n+1}\right)^2$.

The expression for the refraction index of a film is [9,10]

$$n = \frac{\lambda_m\lambda_{m-1}}{2d[\lambda_{m-1} - \lambda_m]}. \quad (3)$$

The ratio of minimum and maximum transmittances in the presence of interference may be presented [10] as

$$\frac{T_{\min}}{T_{\max}} = \left(\frac{2n}{n^2+1}\right) = T_0^2. \quad (4)$$

The spectral dependence of absorptance $\alpha(\lambda)$ for all the three studied ZnO films was obtained by solving Eqs. (1) and (2) numerically with account for relation (4). To determine the optical band gap, absorptance spectrum $\alpha(\lambda)$ of the ZnO film was replotted in coordinates $(\alpha^2 - h\nu)$ [10]. Following this, the values of optical band gap E_g were determined using the transition region linearization method. The film synthesized by pulsed laser ablation has E_g = 3.30 eV. The E_g value for the zinc oxide film synthesized by pulsed electron-beam evaporation is 3.29 eV. The E_g value for the ZnO film formed by reactive ion-plasma sputtering is 3.27 eV.

The photoluminescent properties of thin zinc oxide films synthesized on the quartz substrate using different corpuscular-photonic methods were examined with a Perkin Elmer LS50B luminescence spectrometer at room temperature. The excitation radiation wavelength was 325 nm. The photoluminescence spectra of the studied structures are shown in Fig. 4 (curves *1–3* correspond to the films produced by laser ablation, pulsed electron-beam evaporation, and reactive ion-plasma sputtering, respectively). The

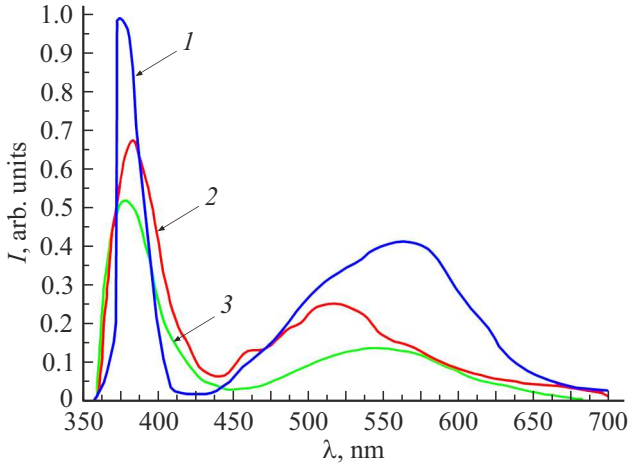

Figure 4. Photoluminescence spectra of ZnO films. The ZnO layer is produced by: *1* — laser ablation; *2* — pulsed electron-beam evaporation; and *3* — reactive ion-plasma sputtering.

photoluminescence spectra of all samples feature an intense luminescence band located in the ultraviolet region near the intrinsic absorption edge of ZnO. According to literature data [11–14], this photoluminescence band is called edge luminescence (EL) that is induced by the emission of various Wannier–Mott excitons.

The luminescence band maximum of the ZnO film synthesized by pulsed laser ablation (Fig. 4, curve *1*) is found at a wavelength of 375 nm and has a half-width of 13 nm. It follows from literature data [12–15] for single-crystal ZnO and thin ZnO films that the photoluminescence lines of donor- or acceptor-bound excitons lie in the spectral band extending from 375 to 400 nm. The UV photoluminescence band of the film fabricated by pulsed electron-beam evaporation (Fig. 4, curve *2*) has the form of a complex curve represented by a sum of two Gaussians with their maxima located at 390 and 400 nm. In addition, this UV photoluminescence band has a 2.8-fold greater half-width and a 1.3-fold lower intensity than the peak of curve *1*. Compared to a similar UV luminescence peak for the zinc oxide film synthesized by laser ablation, the UV photoluminescence peak observed in the film synthesized by electron-beam evaporation is also shifted toward lower energies (longer wavelengths), and its maximum is located at 390 nm. With its increased peak half-width taken into account, the long-wavelength shift of the UV luminescence band maximum in the film formed by electron-beam evaporation relative to the position of the UV maximum in the film produced by laser ablation may be attributed both to the polycrystalline structure of the synthesized film and to the large size of ZnO nanocrystals forming this polycrystalline matrix. The ultraviolet luminescence peak of the film formed by reactive ion-plasma sputtering (Fig. 4, curve *3*) has the form of a bell-shaped asymmetric curve with its maximum positioned at a wavelength of 375 nm. The half-width of this UV luminescence peak

is 2.1 times greater than the half-width of a similar peak for the film synthesized by pulsed laser ablation. The position of the UV photoluminescence maximum for the film obtained by ion-plasma sputtering of the metal target coincides with the position of the UV photoluminescence maximum of the film synthesized by laser ablation. The UV photoluminescence curve reveals an asymmetry in the rise and fall of luminescence intensity: the spectral band of the photoluminescence curve „wing" corresponding to the reduction of intensity is 2.4 times wider than the spectral band of luminescence intensification. This is attributable to the fact that optically active traps involved in UV photoluminescence have a predominant activation energy within the 3.3–2.9 eV range [11,12].

Photoluminescence in the blue-green band of the spectrum has a distinct form in each of the studied zinc oxide films. The film synthesized by pulsed laser ablation has a blue-green photoluminescence band in the form of an asymmetric bell-shaped curve with its increasing section being 1.2 times larger than the „wing" of luminescence decay. It also features the highest intensity among all peaks in the blue-green region of the spectrum, and its maximum reaches 39% of the UV peak intensity. According to literature data [13–15], the traps involved in luminescence of ZnO in the blue-green spectral band are oxygen or zinc vacancies in the bulk of a thin film. Therefore, it is fair to assume that their concentration is the highest in the ZnO film produced by laser ablation. Blue-green luminescence of the film synthesized by pulsed electron-beam evaporation has the form of an asymmetric curve increasing within the 425−510 nm interval and featuring an extended fall region of 525−700 nm. The region of intensification of blue-green photoluminescence may be approximated by a superposition of three Gaussians with their maxima at 463, 480, and 515 nm. The spectral wing of photoluminescence decay has two regions: green and red. The intensity maxima are positioned at 522 and 560 nm. Compared to the photoluminescence intensity of the film produced by laser ablation, the photoluminescence peak of the film formed by electron-beam evaporation is 1.7 times less intense. The intensity of red-band luminescence is 2.6 times lower than the intensity of the blue-green band. This suggests that the concentration of oxygen and zinc vacancies in ZnO films synthesized by electron-beam evaporation is significantly lower than the corresponding concentration in ZnO films fabricated by laser ablation. Luminescence in the blue-green spectral band of the film formed by reactive ion-plasma sputtering of the metal target has the form of a symmetrical bell-shaped curve with a maximum at 550 nm. This curve has no local photoluminescence peaks, suggesting that electrically active bulk defects, which produced photoluminescence observed in the samples examined earlier, are lacking in this film. The peak intensity of the blue-green photoluminescence band of the film synthesized by ion-plasma sputtering is the lowest among all those considered here and is 2.9 times lower than the peak intensity of the blue-green luminescence band of the film synthesized by laser ablation. Thus, it can be assumed that the concentration of optically active traps (oxygen or zinc vacancies) in ZnO films fabricated by reactive ion-plasma sputtering of the metal target is the lowest among the three examined types of films.

Conclusions

All diffraction patterns of the studied zinc oxide films contain a high-intensity diffraction maximum typical of hexagonal zinc oxide (002), which is indicative of a high degree of structural perfection of these films. The high intensity of the (002) peak also provides a clear indication of the presence of a distinct axial texture in all the examined ZnO films in the direction perpendicular to the substrate surface. Shifts of reflection maxima visible in the diffraction patterns of the studied zinc oxide films and changes in their intensity are probably attributable to an increase in the interplanar distance. The sizes of zinc oxide nanocrystallites in the bulk of films synthesized by ion-plasma sputtering, electron-beam evaporation, and laser ablation do not exceed 15, 13, and 11 nm, respectively.

The refraction index of all the examined films is below 2.36. Optical band gap E_g values were determined for all three examined types of zinc oxide films. It turned out that the film synthesized by pulsed laser ablation has $E_g = 3.30$ eV, the film synthesized by pulsed electron-beam evaporation has $E_g = 3.29$ eV, and the film synthesized by reactive ion-plasma sputtering has $E_g = 3.27$ eV.

The photoluminescence spectra of all the examined samples feature an intense luminescence band located in the UV region near the intrinsic absorption edge of ZnO. This UV photoluminescence band is induced by the emission of various Wannier–Mott excitons.

The highest intensity of the UV photoluminescence band was recorded for the ZnO film formed by laser ablation. The maximum of this band is positioned at a wavelength of 375 nm and has a half-width of 13 nm. The UV photoluminescence band of the film fabricated by pulsed electron-beam evaporation has the form of a complex curve represented by a sum of two Gaussians. The maxima of these Gaussians are at 390 and 400 nm. The ultraviolet photoluminescence band of the film obtained by electron-beam evaporation has a 2.8-fold greater half-width and 1.3-fold lower intensity than the UV band of the zinc oxide film obtained by laser ablation. The shift toward lower energies (longer wavelengths) of the 390 nm maximum of UV photoluminescence in the film obtained by electron-beam evaporation should also be noted. With the larger half-width of the peak taken into account, the shift of the UV luminescence band maximum toward longer wavelengths may be attributed both to the polycrystalline structure of the synthesized film and to the large size of ZnO nanocrystallites forming in this film. The ultraviolet luminescence band of the film formed by reactive ion-plasma sputtering of the metal target has the form of a bell-shaped asymmetric curve with a maximum at 375 nm

and a half-width 2.1 times greater than the half-width of a similar peak corresponding to the film synthesized by pulsed laser ablation. The position of the maximum of this UV photoluminescence peak matches the one of a similar UV photoluminescence peak of the film produced by laser ablation. The observed asymmetry of luminescence intensity rise and fall regions is attributable to the fact that optically active traps involved in UV photoluminescence in the ZnO film synthesized by reactive ion-plasma sputtering have a predominant activation energy falling within the range from 3.3 to 2.9 eV.

Having analyzed photoluminescence in the blue-green spectral band in all the studied types of films, we found that the highest concentration of optically active traps (oxygen or zinc vacancies) corresponds to the ZnO film fabricated by laser ablation. The lowest concentration of optically active traps involved in photoluminescence in the blue-green spectral band was observed in the ZnO film synthesized by the reactive ion-plasma method.

A high exciton binding energy and a very short (several nanoseconds) UV photoluminescence decay time enable the use of thin ZnO films in high-speed scintillators and UV photodetectors. In this context, the ZnO film formed on a substrate by pulsed laser ablation is the one most suitable for thin-film scintillators and UV photodetectors of the three studied types of films produced using different corpuscular-photonic methods.

Conflict of interest

The authors declare that they have no conflict of interest.

References

[1] T. Wen-Che, K. Hui-Ling, L. Kun-Hsu. Optics Express, **23** (3), 2187 (2015).
[2] C.L. Wei, Y.E. Chen, C.C. Cheng. Thin Solid Films, **518** (11), 3059 (2010).
[3] B.D. Yao, V.F. Chang, F. Wang. Appl. Phys. Lett., **81** (4), 757 (2002).
[4] O.G. Vendik, Yu.N. Gorin, V.F. Popov. *Korpuskulyarno-fotonnaya tekhnologiya* (Vysshaya Shkola, M., 1984) (in Russian).
[5] A.N. Zakirova, P.N. Krylov, I.A. Suvorov, I.V. Fedotova. Vestn. Udmurt. Gos. Univ. Ser. „Fiz. Kondens. Sostoyaniya Veshchestva,“**4**, 14 (2012) (in Russian).
[6] A.G. Veselov, O.A. Kiryasova, A.A. Serdobintsev. Fiz. Tekh. Poluprovodn., **42** (4), 496 (2008).
[7] A.N. Gruzintsev, V.T. Volkov. Semiconductors, **45** (11), 1420 (2011).
[8] A.A. Rusakov. *Rentgenografiya metallov* (Atomizdat, M., 1977) (in Russian).
[9] Yu.I. Ukhanov. *Opticheskie svoistva poluprovodnikov* (Nauka, M., 1977) (in Russian).
[10] S.A. Alekseev, V.T. Prokopenko, A.D. Yas'kov. *Eksperimental'naya optika poluprovodnikov* (Politekhnika, SPb., 1994) (in Russian).
[11] D.G. Thomas. J. Phys. Chem. Sol., **15**, 86 (1960).
[12] T. Berseth et. al. Appl. Phys. Lett., **89**, 262112 (2006).
[13] Bei Chen Hu, N. Zhou, Q.Y. Zhang, Chung-Yu Ma. Physica Status Solidi (B): **258** (10), 2100024 (2021).
[14] C. Ton-That. Phys. Rev. B, **86**, 115205 (2012).
[15] B.D. Yao, V.F. Chang, F. Wang. Appl. Phys. Lett., **81** (4), 757 (2012).

Translated by D.Safin